Structure of the Viral TAP-Inhibitor ICP47 Induced by Membrane Association[†]

Dirk Beinert,[‡,§] Lars Neumann,[‡] Stephan Uebel,[‡] and Robert Tampé*[,‡,§]

Max-Planck-Institut für Biochemie, Am Klopferspitz 18a, D-82152 Martinsried, Germany, and Lehrstuhl für Biophysik, Technische Universität München, D-85747 Garching, Germany

Received December 2, 1996[⊗]

ABSTRACT: Herpes simplex virus type I protein ICP47 (IE12) turns off antigen presentation by specifically binding to and blocking the major histocompatibility complex- (MHC-) encoded transporter associated with antigen processing (TAP). Due to the lack of translocated peptides inside the endoplasmic reticulum, MHC class I molecules fail to assemble and therefore MHC−peptide complexes do not reach the cell surface for immune recognition by cytotoxic T-lymphocytes. Here we investigated the structure of ICP47 representing the first natural inhibitor of an ATP-binding-cassette (ABC) transporter identified so far. First, we demonstrate that the N-terminal half of ICP47 is as active in inhibition of human TAP as the full-length protein and therefore serves as an ideal model to investigate structural and functional aspects of the inhibitor. Second, from circular dichroism analysis, the viral inhibitor of TAP appears to be mainly unstructured in aqueous solution. However, in the presence of membrane mimetics or lipid membranes an α-helical structure is induced. Third, circular dichroism and fluorescence spectroscopy reveal that membrane adsorption and conformational change of ICP47 are directly dependent on the surface charge density of the lipid membrane. Therefore we conclude that docking to membranes induces a conformational change in ICP47 that may be prerequisite to blocking TAP function.

The recognition of a virus-infected cell by T-lymphocytes is strongly dependent on the presentation of fragments derived from viral proteins in association with major histocompatibility complex (MHC) class I molecules (Townsend & Bodmer, 1989). The majority of these antigenic peptides are generated by protein degradation in the cytosol or nucleus. These peptides are translocated into the endoplasmic reticulum (ER) lumen by the MHC-encoded transporter associated with antigen presentation (TAP), where they are needed for correct assembly of MHC molecules (Howard, 1995). Subsequently, peptide-loaded MHC class I molecules leave the ER and present their peptide on the cell surface to cytotoxic T-lymphocytes (Jackson & Peterson, 1993; Yewdell & Bennink, 1992).

In vitro assays using permeabilized cells (Neefjes et al., 1993; Androlewicz et al., 1993) or isolated microsomes from mammalian cells (Shepherd et al., 1993) gave strong evidence that peptide transport into the ER lumen was ATP- and TAP-dependent. Heterologous expression of TAP in insect cells demonstrated that this membrane protein complex mediates peptide transport across the microsomal membrane even in the absence of cofactors derived from a highly developed immune system (Meyer et al., 1994). The transport mechanism of TAP could be dissected into two steps (van Endert et al., 1994). First, peptide binding to TAP was shown to be specific and ATP-independent (Androlewicz & Cresswell, 1994; van Endert et al., 1994; Uebel et al., 1995), whereas TAP binds ATP even in the absence of peptides (Müller et al., 1994; Russ et al., 1995). Second, peptide translocation is strictly ATP-dependent (Neefjes et al., 1993; Androlewicz et al., 1993; Shepherd et al., 1993).

It is obvious that persistent viruses are forced to evade immune surveillance for survival. The Adenoviridae and Herpesviridae have been discovered to intervene specifically with MHC class I-restricted antigen presentation (Hill & Ploegh, 1995). Herpes simplex virus type I DNA codes for an immediate early protein ICP47 (IE12), which was shown to block surface expression of MHC class I molecules (York et al., 1994). It has been demonstrated that this viral protein prevents peptide translocation into the ER lumen by specifically interacting with human TAP. Therefore, assembly and trafficking of MHC class I molecules is impaired (Früh et al., 1995; Hill et al., 1995). Recently, we and others were able to demonstrate that purified ICP47 inhibits peptide import into insect cell microsomes by preventing peptide binding to the human TAP complex (Ahn et al., 1996; Tomazin et al., 1996).

TAP is a member of the evolutionarily highly conserved superfamily of ABC transporters found in bacteria (Fath & Kolter, 1993), in archaea (Bult et al., 1996), and in eukarya (Higgins, 1992). Prominent members of the ABC family include the human P-glycoprotein and the multidrug resistance-associated protein (Mrp), both of which confer a multidrug resistance phenotype upon overexpression. Further, the cystic fibrosis transmembrane conductance regulator (CFTR), the peroxisomal membrane proteins PMP70 and ALDP (adrenoleukodystrophy protein), and the human sulfonylurea receptor (SUR) represent mammalian ABC proteins of medical importance. Another example involved in human pathogenesis, HlyB of *Escherichia coli* is responsible for the secretion of α-hemolysin (HlyA), which is targeted to the extracellular medium by its C-terminal signal sequence (Holland et al., 1990).

Here, the structure of a natural inhibitor of an ABC transporter was investigated for the first time. In the presence of membrane mimetics or lipid membranes, a drastic conformational change of ICP47 from a random-coil into

[†] This work was supported by the Deutsche Forschungsgemeinschaft.

* Corresponding author. Phone: 0049-89-8578-2646. Fax: 0049-89-8578-2641. E-mail: tampe@vms.biochem.mpg.de.

[‡] Max-Planck-Institut für Biochemie.

[§] Technische Universität München.

[⊗] Abstract published in *Advance ACS Abstracts,* April 1, 1997.

S0006-2960(96)02940-6 CCC: $14.00

an α-helical structure was observed. We further demonstrate that membrane adsorption and conformational change of ICP47 are promoted by negatively charged phospholipids. These interactions with membranes might be the initial steps by which the viral inhibitor assembles with the TAP complex and blocks its function.

MATERIALS AND METHODS

Materials. All phospholipids, including dimyristoyl-L-α-phosphatidylcholine (DMPC), palmitoyloleyl-L-α-phosphatidylcholine (POPC), dimyristoyl-L-α-phosphatidylglycerol (DMPG), dilauryl-L-α-phosphatidic acid (DLPA), and dimyristoyl-L-α-phosphatidic acid (DMPA) were purchased from Avanti Polar Lipids. Dihexadecyldimethylammonium bromide (DHDAB) was ordered from Aldrich (Steinheim, Germany). The purity of the lipids was controlled by thin-layer chromatography. The phosphate buffer (Na_2HPO_4/NaH_2PO_4) was adjusted to pH 7.0 and stored at 4 °C until use. Aqueous solutions were filtered through a Millex-GV sterilizing filter unit before use (0.22 μm diameter pores; Millipore S. A., Molsheim, France). Trifluoroethanol (TFE) and sodium dodecyl sulfate (SDS) were the highest quality available (Sigma, Deisenhofen, Germany).

Isolation of Full-Length and Truncated ICP47. Full-length ICP47 containing an additional hexahistidine tag at the N-terminus was expressed in *E. coli* and purified by metal affinity chromatography and reversed-phase HPLC as described previously (Ahn et al., 1996). The purity of the protein was verified by SDS−PAGE and HPLC. Truncated ICP47(1−53) MSWALEMADTFLDNMRVGPRTYADVRDEIN KRGREDREAARTAVHDPERPLLR was synthesized on a multiple peptide synthesizer (MultiSynTech, Bochum, Germany) by conventional Fmoc chemistry and purified by preparative HPLC using a reversed-phase C_{18} column. The purity of ICP47(1−53) was found to be >95% according to analytical reversed-phase HPLC. Identity of ICP47(1−53) was verified by mass spectrometry. Protein concentrations were determined using the MicroBCA protein assay (Pierce, Rockford, IL).

Preparation of TAP-Containing Insect Cell Microsomes. The heterologous expression of human TAP in insect cells has been reported previously (Meyer et al., 1994). Insect cell microsomes were prepared by a combination of differential and sucrose gradient centrifugation as described in detail (Meyer et al., 1994). Isolated microsomes were resuspended in PBS/1 mM DTT, snap-frozen in liquid nitrogen, and stored at −80 °C.

TAP Inhibition Assay. TAP-containing microsomes were diluted with assay buffer [PBS with 1 mg/mL dialyzed bovine serum albumin, 1 mM DTT, 2 mM $MgCl_2$, and 0.05% poly(ethylene glycol)] to a final protein concentration of 25 μg/mL and the were homogenized by drawing through a 23 gauge needle. From this suspension, 150 μL was incubated with 100 nM radiolabeled peptide RRYQKSTEL and the appropriate amount of unlabeled competitor for 45 min at 4° C. Thereafter, 350 μL of ice-cold assay buffer was added and the microsomes were pelleted by centrifugation (8 min, 12000*g* at 4 °C). Vesicle-associated radioactivity was quantified by γ-counting after one washing step with 500 μL of ice-cold assay buffer. The amount of bound peptide was corrected for nonspecific binding in the presence of a 400-fold excess of unlabeled peptide. The data set was fitted by the competition equation (Uebel et al., 1995) and the concentration needed for 50% inhibition (IC_{50}) was determined from at least three independent competition assays. Peptide synthesis and the radiolabeling procedure have been described previously (Uebel et al., 1995).

Vesicle Preparation. Stock solutions of different lipids in chloroform/methanol (3/1) were mixed, yielding the appropriate molar lipid ratio. The organic solvent was evaporated under N_2 flow. The remaining lipid film was dried under vacuum. The lipid film was hydrated in 50 mM phosphate buffer (pH 7.0) and sonicated using a Branson W-250 microtip sonifier at a frequency of 20 kHz with a generator output of only 40 W to reduce cavity effects. During sonification (duty cycle 50% for 5 min, duty cycle 100% for 1 min), samples were kept at a constant temperature above lipid phase transition. Before measurement, the transparent vesicle suspension was centrifuged for 10 min at 23000*g* to eliminate metal contamination. To prevent phase transition effects, samples were equilibrated at the temperature used in the experiment. The average vesicle dimensions were measured to be 80 nm in diameter by dynamic light scattering and electron microscopy.

Circular Dichroism Spectroscopy. CD spectra were recorded on an Auto Dichrograph Mark IV (ISA Jobin Yvon) using a 1 mm Quartz-Suprasil cuvette (Hellma, Müllheim, Germany). The temperature of the samples was controlled by a circulating water bath. Vesicles were prepared 1 h before data acquisition and ICP47 was incubated at least 45 min before measurement to allow binding. This period is necessary to approach equilibrium and has previously been determined through binding assays. The protein and lipid concentrations were adjusted to 16 μM and 3.0 mM, respectively. Each spectrum was the average of 10 scans from 195 to 250 nm wavelength with 0.1 nm steps and an integration time of 0.1 s. All spectra were background-corrected for spectra obtained from the same solution without protein. CD spectra were smoothed and converted to mean residue ellipticity $[\Phi]_m$ (deg cm^2 dmol^{-1}). The ratio of the secondary structure (α-helix, β-sheet, or random coil) was analyzed mathematically by using the CONTIN fit (Provencher & Glöckner, 1989) or graphically by using the ellipticity at 222 nm characteristic for α-helical proteins.

Fluorescence Spectroscopy. The tryptophan fluorescence was recorded using a Fluorolog-2 fluorescence spectrometer and dM3000 software (SPEX Industries, Edison, NJ). The fluorescence of the tryptophan residue at position 3 of ICP47 was excited at 290 nm and the emission spectrum was recorded from 315 to 500 nm. The temperature of the samples was controlled by a circulating water bath. For direct comparison, the same samples have been analyzed by CD spectroscopy. The protein or lipid concentration was adjusted to 5.8 μM or 1.1 mM, respectively.

RESULTS

N-Terminal Fragment Embodies the Active Domain of ICP47. In order to facilitate the structural analysis, we first investigated whether a truncated fragment of ICP47 remains fully active in inhibition of human TAP. In this respect, we performed inhibition studies with systematic scans of overlapping fragments derived from ICP47. All of these 25-mer peptides were found to be inactive, suggesting that a larger domain including certain structural characteristics is

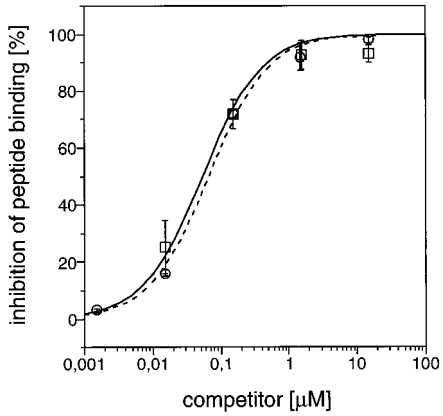

FIGURE 1: Activity of truncated and full-length ICP47. Peptide binding of radiolabeled peptide (100 nM RRYQKSTEL) to insect cell microsomes containing human TAP was analyzed at various concentrations of full-length His-ICP47 (squares) or truncated ICP47(1−53) (circles) at 4 °C. All data were obtained by duplicate or triplicate measurements (error bars: ±SD) and fitted by the competitor curve as described (Uebel et al., 1995), leading to an affinity constant of 50 nM for His-ICP47 (solid line) and 60 nM for ICP47(1−53) (dashed line), respectively. Within the range of error, the binding constants for full-length and truncated ICP47 are identical.

required to block peptide binding to the TAP complex (S.U. and R.T., unpublished results). Sequence comparison of ICP47 derived from various virus strains (Watson et al., 1981; Whitton & Clements, 1984; McGeoch et al., 1985, Koszinowski, personal communication) revealed a highly conserved N-terminal region within residues 1−52. Therefore we speculate that this conserved region might cover the active domain of the viral TAP inhibitor. In order to address the question experimentally, we synthesized ICP47(1−53) by solid-phase techniques and purified the fragment by reversed-phase chromatography. The C-terminal arginine (position 53) was attached to increase the solubility of the synthetic product. Using a TAP inhibition assay as previously described (Ahn et al., 1996), we compared the activity of this fragment with the full-length protein expressed in *E. coli*. As summarized in Figure 1, we found the truncated ICP47(1−53) to be fully active with respect to inhibition of peptide binding to human TAP. The binding constants of His-ICP47 and ICP47(1−53) for human TAP appear to be identical and were determined to be 50 and 60 nM, respectively. So we conclude that ICP47(1−53), lacking the redundant N-terminal fusion tag and the C-terminal domain, covers the active domain of the TAP inhibitor. Thus, this fragment represents an ideal model to investigate structural and mechanistic aspects of this pathogenic factor.

ICP47 Is Mainly Unstructured in Aqueous Solution. The relevance of a larger sequence region of ICP47 required for inhibition of TAP implies that a higher structural order of the viral protein may be critical for its activity. Therefore, we investigated the secondary structure of ICP47(1−53) by means of circular dichroism spectroscopy. Surprisingly, the CD spectrum of ICP47(1−53) shows no characteristics of secondary structure in phosphate buffer (Figure 2a). The same result was obtained for full-length His-ICP47 (not shown). Screening for conditions that support protein folding, we studied the influence of protein concentration and different pH values on the secondary structure of ICP47(1−53). Protein concentrations from the detection limit of 0.05 mg/mL up to 0.4 mg/mL and pH values

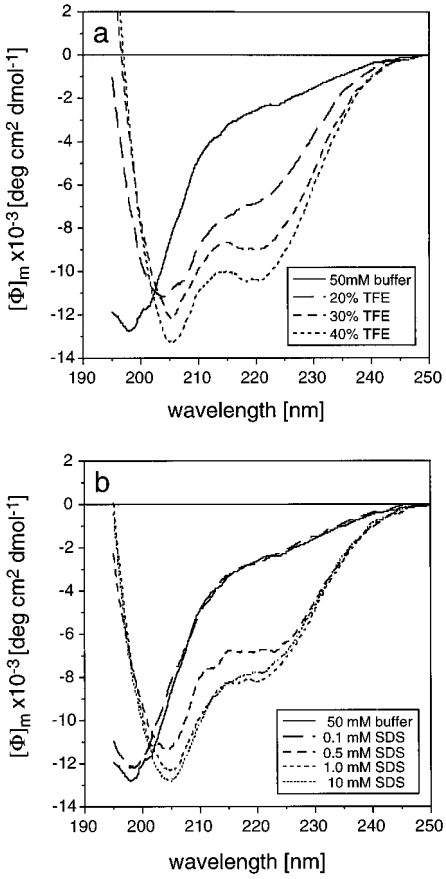

FIGURE 2: Circular dichroism of ICP47(1−53) in aqueous solution at different concentrations of TFE (a) or SDS (b). The secondary structure of ICP47(1−53) was analyzed by CD spectroscopy at 20 °C as described in Materials and Methods. The protein concentration was adjusted to 0.1 mg/mL (16 μM) in 50 mM sodium phosphate buffer (pH 7.0) containing increasing concentrations of TFE (percent vol/vol) or SDS (millimolar).

reaching from 5.0 to 9.0 did not influence the secondary structure of ICP47(1−53) (not shown). Therefore, it is highly unlikely that a conflicting charge distribution in the protein causes unfolding. However, secondary structure predictions suggest that ICP47(1−53) contains two α-helical regions spanning positions 3−13 and 35−43. Earlier observations in our group demonstrated that ICP47 is very hydrophobic and dissolving it in organic solvents does not abolish its activity. This led to the speculation that ICP47 might assume a higher structural order in a lipidlike environment.

Membrane Mimetics Induce an α-Helical Structure of ICP47. It is known that an apolar environment can stabilize the α-helical structure of N-terminal signal peptides for protein secretion, which appear also to be unstructured in aqueous solution (Gierasch, 1989). To imitate such a lipid environment, we first analyzed the secondary structure of ICP47(1−53) in the presence of various membrane mimetics such as trifluoroethanol (TFE) or sodium dodecyl sulfate (SDS). Starting from a random-coil structure in aqueous solution, drastic changes of the secondary structure were observed with increasing concentrations of TFE. The CD spectra developed a characteristic minimum at 206 nm and a shoulder at 222 nm at the expense of the minimum at 198 nm, indicating that TFE induces an α-helical conformation in the active domain of viral inhibitor (Figure 2a). The spectra and the α-helical content do not change significantly

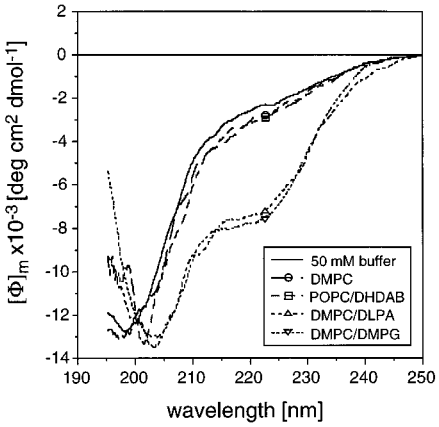

FIGURE 3: Circular dichroism of ICP47(1−53) in the presence of lipid membranes. CD spectra of 16 μM ICP47(1−53) were recorded in 50 mM sodium phosphate buffer (pH 7.0) and in the presence of various lipid vesicles. Small unilamellar vesicles were prepared from neutral lipids (DMPC), equimolar mixtures of POPC and the positively charged lipid (DHDAB), or equimolar mixtures of DMPC and different negatively charged lipids (DLPA or DMPG). The final lipid concentration was kept constant (3 mM). All spectra are background-subtracted using the same vesicle preparation in the absence of protein. The vesicles are prepared as described in Materials and Methods.

above 40% (v/v) TFE. Again, similar results were obtained for the recombinant full-length His-ICP47 (not shown). Since truncated and full-length protein behave similarly with respect to structural changes observed in aqueous versus lipidlike environments, we concluded that the fragment covers not only the active domain but also the region underlying structural reorganization.

In addition to this we studied the secondary structure of ICP47(1−53) in the presence of SDS micelles, which provide a simple hydrophobic/ hydrophilic interface related to membranes. Here, a drastic conformational change from a random coil to an α-helical structure was observed (Figure 2b). When the SDS concentration drops below the critical value of about 1.0 mM, the α-helical dichroism is reduced. Above that SDS concentration, the CD spectra remain constant.

Negatively Charged Membranes Promote Helical Structure of ICP47. Membrane mimetics such as TFE or SDS have the intrinsic property of inducing α-helical conformation of peptides *per se*. To avoid an overestimation of such effects, we analyzed the secondary structure of ICP47 in the presence of lipid membranes. As summarized in Figure 3, lipid vesicles that contain negatively charged lipids, such as phosphatidic acid (PA), phosphatidylglycerol (PG), or phosphatidylserine (PS) (latter not shown), induce an α-helical conformation, whereas neutral or positively charged lipid vesicles, such as phosphatidylcholine (DMPC or POPC) or dihexadecyldimethylammonium bromide (DHDAB), hardly affect the secondary structure of ICP47(1−53). Therefore, we conclude that the viral TAP inhibitor adopts a more α-helical structure when bound to membranes and that negatively charged lipids induce membrane adsorption and conformational change.

To investigate the effect of the membrane charge density in more detail, we chose neutral DMPC vesicles doped with various ratios of negatively charged DMPG. These mixtures were found to be ideal, since these lipids do not phase-segregate over the entire mixing range. Furthermore, due to the main phase-transition temperatures of 23.5 °C (DMPC)

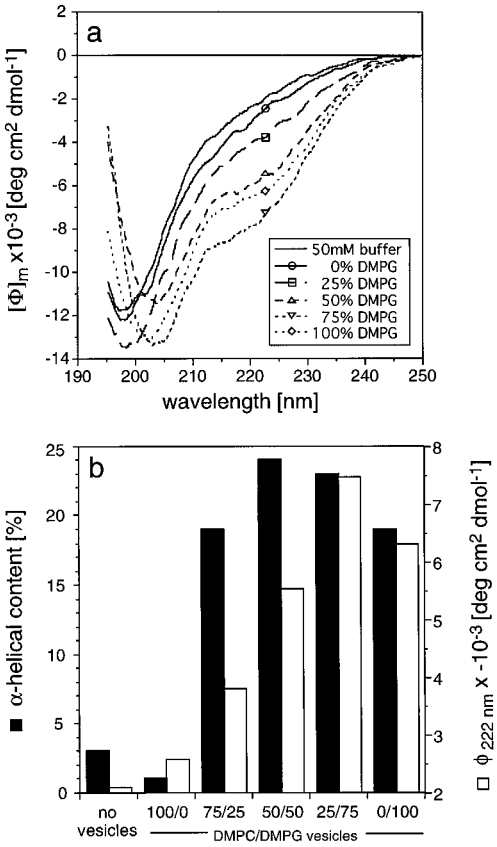

FIGURE 4: Helical structure of ICP47(1−53) is induced by negatively charged lipids. Using circular dichroism spectroscopy, the influence of negatively charged lipids on the secondary structure of ICP47 was investigated. The protein and lipid concentration were adjusted to 16 μM and 3 mM, respectively. Experiments were performed in 50 mM phosphate buffer (pH 7.0) at 37 °C (a). The vesicles were prepared as described in Materials and Methods. For different conditions, the α-helical content of ICP47(1−53) was estimated by a CONTIN fit or by the molar ellipticity at 222 nm (b).

and 24 °C (DMPG), membrane adsorption and the conformational change of ICP47 can be analyzed at different temperatures, where the membrane is in either a crystalline or a fluid state. In comparison to CD spectra obtained in pure phosphate buffer, no drastic changes, besides slight shoulders at 206 and 222 nm, were observed in the presence of pure DMPC vesicles. With increasing molar ratios of DMPG, a profound increase of the α-helical content was detected at 37 °C (Figure 4a). At different DMPC/DMPG ratios the helical content of ICP47(1−53) was estimated using the CONTIN fit or comparison of the ellipticity at 222 nm, which is characteristic for α-helices (Figure 4b). Due to this analysis, ICP47(1−53) appears to be mainly unstructured in aqueous solution (3% α-helical content). However, with increasing negative charge density of the lipid vesicles, a more and more α-helical structure is formed, reaching a plateau (20−25% α-helix) at 25−50 mol % DMPG. At higher molar ratios of DMPG, this effect is reverted. In comparison to these experiments performed at 37 °C, we observed similar conformational changes of ICP47(1−53) induced by negatively charged lipids at 20 and 10 °C, although the lipid bilayer is in a crystalline state. Since incorporation of α-helices into a crystalline, densely packed lipid layer is energetically as well as sterically highly disfavored, we conclude that ICP47 adsorbs to the outer

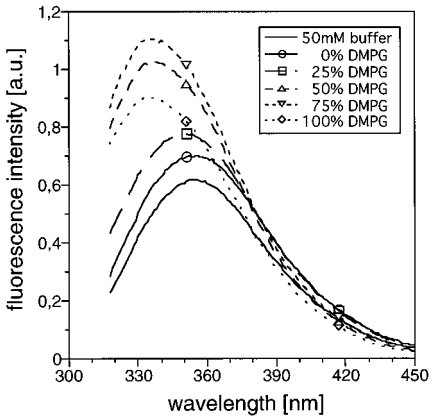

FIGURE 5: Bathochromic shift of the tryptophan fluorescence of ICP47(1−53) in the presence of negatively charged lipid vesicles. The tryptophan fluorescence (λ_{ex}= 290 nm) of ICP47(1−53) was recorded from 315 to 500 nm at 37 °C. The protein and lipid concentrations were 5.8 μM and 1.1 mM, respectively. The molar ratio of DMPC and DMPG was varied from 0 to 1. All spectra are background-subtracted using an identical vesicle preparation in the absence of protein.

membrane leaflet rather than incorporating into the lipid bilayer.

Adsorption of ICP47 to Negatively Charged Membranes. ICP47 contains a single tryptophan residue at position 3, directly adjacent to the predicted α-helix (3−13). If we assume that this α-helix is responsible for membrane adsorption and conformational change, then this tryptophan would serve as an ideal probe for ICP47 membrane interaction. Thus we have analyzed the tryptophan fluorescence of ICP47(1−53) in aqueous solution and in the presence of lipid vesicles at various temperatures. At 10 and 37 °C, the fluorescence emission has its maximum at 355 nm, indicating that the tryptophan is completely solvent exposed (Figure 5). While hydrophobic side chains are usually buried in folded domains, the fluorescence data give further evidence that ICP47 is highly dynamic and mainly unstructured in aqueous solution. After addition of pure DMPC vesicles at 20 °C, the wavelength of the emission maximum remains constant and the fluorescence intensity increases slightly, reflecting only a very weak interaction of ICP47(1−53) with neutral changed phospholipids. By increasing the molar ratio of DMPG/DMPC vesicles, we observed drastic changes of the fluorescence emission. The emission maximum was shifted to 335 nm and the fluorescence intensity increased 2-fold. The changes of the secondary structure observed in different lipid charge densities are in very good agreement with the changes in tryptophan fluorescence. Maximum changes of the fluorescence intensity were observed at 50 mol % DMPG, whereas a slight opposite effect was detected at 100 mol % DMPG. Similar fluorescence spectra were recorded at 10 and 37 °C, indicating that the adsorption process is not strongly influenced by the physical state of the lipid bilayer.

DISCUSSION

The immediate early protein IE12 (ICP47) plays a key role in the persistence of Herpes simplex virus. HSV-ICP47 binds specifically to the MHC-encoded peptide transport complex (TAP1·TAP2), thereby blocking the supply of peptide for the correct assembly and trafficking of MHC class I molecules. Consequently, the antigen presentation is turned off and the infected cells are masked from immune recognition. In the present study we have investigated structural aspects of the viral TAP inhibitor by means of TAP inhibition assays, circular dichroism analysis, and fluorescence spectroscopy. We report that an N-terminal fragment of ICP47 retains full activity in comparison to the full-length protein, demonstrating that the active domain of ICP47 is covered by the first 53 amino acid residues. Since this synthetic fragment lacks the apparently redundant C-terminal half and a fusion tag used for purification of the recombinant full-length protein, it serves as an ideal model to investigate structural and mechanistic aspects of the viral TAP inhibitor. Fragments (25-mers) stepwise overlapping the sequence of ICP47 were found to be completely inactive. Thus we conclude that a larger domain of ICP47 is required to retain full activity and that a higher structural order of the active domain might be involved in TAP inhibition. Surprisingly, the full-length protein as well as its active fragment ICP47(1−53) appears to be mainly unstructured in aqueous solution as observed by circular dichroism analysis. Since variation of the protein concentration (0.05−0.4 mg/mL) and pH value (5.0−9.0) did not affect the secondary structure, we can exclude that high protein concentrations or a certain pH value are responsible for a lack of a defined structure by intermolecular interaction.

However, in the presence of membrane mimetics, a drastic conformational change of ICP47 to a more α-helical structure was observed. This result is in line with secondary structure predictions, which propose two helices located within residues 3−13 and 35−43 (Figure 6a). From the CD spectra obtained in 40% TFE, we calculated an α-helical content of about 40−50% for ICP47(1−53), which was not significantly increased at higher TFE concentrations. Therefore, we conclude that both predicted α-helices are formed under these conditions. A conformational change of ICP47 is already observed at low TFE concentrations, indicating a high helical propensity of the viral inhibitor (Nelson & Kallenbach, 1989).

Because the interaction of TFE with proteins or peptides is poorly understood so far, we investigated the secondary structure of ICP47(1−53) in buffer containing various concentrations of the ionic detergent SDS. Helix formation starts above 0.1 mM SDS and is completed at 1 mM SDS. No further conformational changes are observed above 1 mM SDS or below 0.1 mM SDS. That the transition occurs in a narrow concentration range of the detergent can be explained in two ways: (i) the critical factor for helix formation might be the presence of SDS micelles which are only formed above the critical micellar concentration (cmc). Using dynamic light scattering, we could demonstrate that under these experimental conditions micelles start to form in this concentration range. (ii) About 60 SDS molecules typically built up one detergent micelle depending on the ionic strength, pH value, and presence of other amphipathic molecules. At 1 mM SDS we can calculate that at least every inhibitor molecule is bound to one micelle and therefore saturation has occurred. Taken together, both effects can account for the SDS-dependent conformational change of ICP47(1−53). However, the second explanation seems unlikely because the transition happened more or less spontaneously rather than following a Langmuir isotherm expected for protein adsorption to interfaces.

Strong support for the biological relevance of the conformational change of ICP47 was obtained by CD analysis of

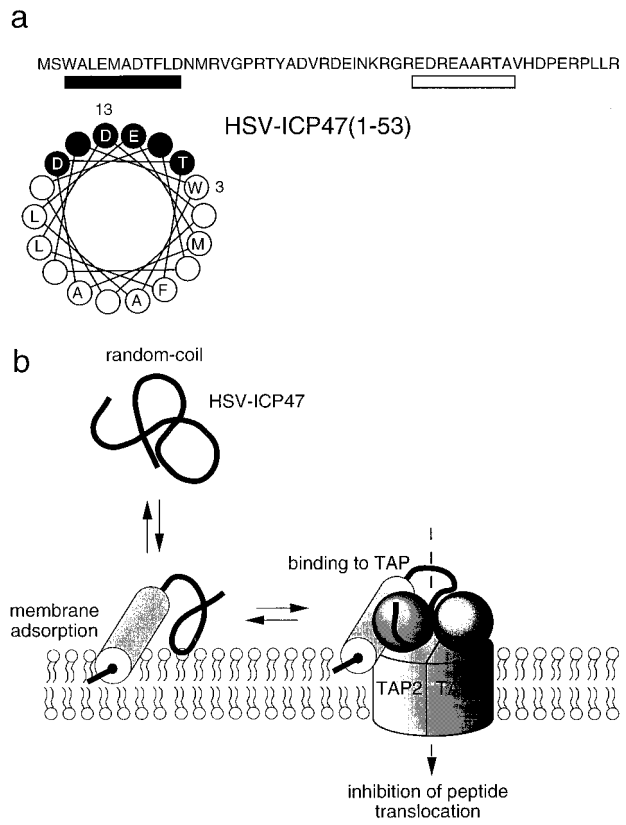

FIGURE 6: Model illustrating the structure, membrane adsorption, and conformational change of the viral TAP inhbititor. (a) The secondary structure was independently predicted using programs of the Genetic Computer Group (GCG, Madison, WI) and MacMatch 1.1d (Scott Presnell, UCSF, Ca). The first predicted α-helix of ICP47 is shown in an α-helical wheel representation, underlining its amphipathic character. (b) Model of the membrane interaction and specific blocking of TAP function by ICP47.

ICP47(1−53) in the presence of lipid membranes. As summarized in Figure 3, only negatively charged lipids contribute to the helical conformation of the viral inhibitor. Furthermore, this effect is not restricted to a single type of lipid head group or lipid chain length. Thus we conclude that the charge density in the lipid bilayer is the critical factor for ICP47−membrane interaction. To support the biological relevance of our studies, we investigated the α-helical content of ICP47(1−53) in more detail using mixtures of the neutral lipid DMPC and the negatively charged lipid DMPG. The data reflect a strong increase of the α-helical content above 25 mol % DMPG, which correlates with the amount of negatively charged lipids found in the ER membrane [48% phosphatidylcholine, 24% phosphatidylethanolamine, 12% phosphatidylinositol, 5% phosphatidylserine, 5% sphingomyeline, 6% other, summed up to 22% negative lipids (Yorek, 1993)]. From the CONTIN fit or the ellipticity at 222 nm, the α-helical content of ICP47(1−53) was calculated to a maximum of 20−25% in the presence of negatively charged membranes or SDS, indicating that only one of the two predicted α-helices is formed. Unpublished data of our group demonstrate that the deletion of the first α-helix causes complete inactivation and loss of an induced α-helical structure of the viral inhibitor, whereas deletion of the second predicted α-helix only decreases the binding affinity for TAP (L.N. and R.T., unpublished results). Therefore, we propose that the N-terminal region forms an α-helix required for membrane anchoring and TAP inhibition. Interestingly, the first predicted α-helix is amphipathic, composed of a hydrophilic face as illustrated by an α-helical wheel (Figure 6a).

Further evidence for specific docking of the predicted α-helix to negatively charged membranes was obtained by fluorescence spectroscopy. Here, tryptophan located at position 3 (Figure 6B) served as a reporter molecule to study the membrane interaction of this N-terminal region. Tryptophan is often found at the ends of membrane helices within the interfacial region and could therefore serve as a membrane anchor. In the presence of negatively charged membrane vesicles, a drastic increase of the fluorescence intensity and a bathochromic shift of the fluorescence maximum were observed. These data support the results obtained by secondary structure analysis. ICP47 is mainly unstructured in aqueous solution and the tryptophan residue is not buried in a folded cavity. Tryptophan is located in a hydrophilic environment (λ_{max} = 350 nm) and the fluorescence is efficiently quenched by collision with water molecules. In the presence of negatively charged lipids, tryptophan senses the lipid environment (λ_{max} = 335 nm), and due to membrane adsorption, quenching by water is less efficient. Membrane docking and helix formation is also induced if the membrane is in a crystalline state, indicating that the amphipathic helix might adsorb to the outer leaflet rather than incorporating into the lipid bilayer, which would be energetically highly disfavored at these phase conditions.

It is interesting to note that adsorption of a negatively charged amphipathic α-helix is promoted by a negatively charged lipid interface. However, membrane partitioning is a complex function of the membrane affinity and the potential for secondary structure formation (Deber & Goto, 1996; Wimley et al., 1996). Polypeptides whose solvation energies of the peptide side chain and backbone promote partitioning will adsorb to the membrane and undergo transition from random aqueous-based structures to intramolecularly hydrogen-bonded structures at the membrane interface. This effect has been widely observed for signal sequences (Gierasch, 1989; Tamm, 1991) and for various peptide hormones (Schwyzer, 1995).

Bacterial ABC transporters such as hemolysin B (HlyB) are responsible for nonclassical secretion of various toxins including α-hemolysin, proteases, and lipases. These substrates are recognized by a topogenic, nonclassical secretion signal at the C-terminus covered by 50−70 amino acids. Although the C-termini of different signal sequences are not sequence-related, they are functionally equivalent and heterologous complementation between them has been reported (Zhang et al., 1993). Furthermore, deletions within the C-terminal signal region cause severe reduction in HlyA transport; however, point mutations have failed to identify a discrete, continuous sequence responsible for recognition and subsequent translocation (Kenny et al., 1992; Stanley et al., 1991). CD analysis and NMR spectroscopy revealed that the signal sequences of *E. coli* α-hemolysin and *Pasteurella* leukotoxin are highly unstructured in aqueous solution, whereas a more α-helical structure is formed in the presence of TFE, SDS, or negatively charged lipids (Sheps et al., 1995; Yin et al., 1995; Zhang et al., 1995). Interestingly, these results are similar to the finding obtained for the unrelated viral inhibitor of TAP, which represents a polypeptide of similar length and similar predicted secondary structure.

We therefore propose the following model of ICP47-mediated blocking of TAP function (Figure 6b): By docking to the membrane, the viral inhibitor, similar to other nonclassical bacterial secretion signals, changes its conformation from a random coil to an α-helical structure. It is tempting to speculate that these membrane-induced structural changes might be a key recognition element for subsequent binding to TAP or other ABC transporters.

ACKNOWLEDGMENT

We thank Dr. L. Moroder and Mrs. E. Weyher-Stingl (Bioorganic Chemistry, MPI for Biochemistry) for the use of the CD spectrometer. We are indebted to Dr. G. Jung and Mr. W. Kraas (Organic Chemistry, University of Tübingen) for peptide synthesis and mass spectroscopy. We are grateful to Stefanie Urlinger, Titja Plantinga, and Anja Jestel for critical reading and comments.

REFERENCES

Ahn, K., Meyer, T. H., Uebel, S., Sempé, P., Djaballah, H., Yang, Y., Peterson, P. A., Fruh, K., & Tampé, R. (1996) *EMBO J. 15*, 3247−3255.

Androlewicz, M. J., & Cresswell, P. (1994) *Immunity 1*, 7−14.

Androlewicz, M. J., Anderson, K. S., & Cresswell, P. (1993) *Proc. Natl. Acad. Sci. U.S.A. 90*, 9130−9134.

Bult, C. J., White, O., Zhou, L., Fleischmann, R. D., Sutton, G. G., Balke, J. A., Fitz-Gerald, L. M., Clayton, R. A., Gocayne, J. D., Kerlavage, A. R., Dougherty, B. A., Tomb, J.-F., Adams, M. D., Reich, C. I., Overbeek, R., Kirkness, E. F., Weinstock, K. G., Merrick, J. M., Glodek, A., Scott, J. L., Geoghagen, N. S. M., Weidman, J. F., Fuhrmann, J. L., Nguyen, D., Utterback, T. R., Kelley, J. M., Peterson, J. D., Sadow, P. W., Hanna, M. C., Cotton, M. D., Roberts, K. M., Hurst, M. A., Kaine, B. P., Borodovsky, M., Klenk, H.-P., Fraser, C. M., Smith, H. O., Woese, C. R., & Venter, J. C. (1996) *Science 273*, 1058−1072.

Deber, C. M., & Goto, N. K. (1996) *Nat. Struct. Biol. 3*, 815−818.

Fath, M. J., & Kolter, R. (1993) *Microbiol. Rev. 57*, 995−1017.

Früh, K., Ahn, K., Djaballah, H., Sempé, P., Van Endert, P. M., Tampé, R., Peterson, P. A., & Yang, Y. (1995) *Nature 375*, 415−418.

Gierasch, L. M. (1989) *Biochemistry 28*, 923−930.

Higgins, C. F. (1992) *Annu. Rev. Cell Biol. 8*, 67−113.

Hill, A., & Ploegh, H. (1995) *Proc. Natl. Acad. Sci. U.S.A. 92*, 341−343.

Hill, A., Jugovic, P., York, I., Russ, G., Bennink, J., Yewdell, J., Ploegh, H., & Johnson, D. (1995) *Nature 375*, 411−415.

Holland, I. B., Kenny, B., & Blight, M. (1990) *Biochimie 72*, 131−141.

Howard, J. C. (1995) *Curr. Opin. Immunol. 7*, 69−76.

Jackson, M. R., & Peterson, P. A. (1993) *Annu. Rev. Cell Biol. 9*, 207−235.

Kenny, B., Taylor, S., & Holland, I. B. (1992) *Mol. Microbiol. 6*, 1477−1489.

McGeoch, D. J., Dolan, A., Donald, S., & Rixon, F. J. (1985) *J. Mol. Biol. 181*, 1−13.

Meyer, T. H., Van Endert, P. M., Uebel, S., Ehring, B., & Tampé, R. (1994) *FEBS Lett. 351*, 443−447.

Müller, K. M., Ebensperger, C., & Tampé, R. (1994) *J. Biol. Chem. 269*, 14032−14037.

Neefjes, J. J., Momburg, F., & Hämmerling, G. J. (1993) *Science 261*, 769−71.

Nelson, J. W., & Kallenbach, N. R. (1989) *Biochemistry 28*, 5256−5261.

Provencher, S. W., & Glöckner, J. (1989) *Biochemistry 20*, 33−37.

Russ, G., Esquivel, F., Yewdell, J. W., Cresswell, P., Spies, T., & Bennick, J. R. (1995) *J. Biol. Chem. 270*, 21312−21318.

Schwyzer, R. (1995) *Biopolymers 37*, 5−16.

Shepherd, J. C., Schumacher, T. N., Ashton-Rickardt, P. G., Imaeda, S., Ploegh, H. L., Janeway, C. A., Jr., & Tonegawa, S. (1993) *Cell 74*, 577−584.

Sheps, J. A., Cheung, I., & Ling, V. (1995) *J. Biol. Chem. 270*, 14829−14834.

Stanley, P., Koronakis, V., & Hughes, C. (1991) *Mol. Microbiol. 5*, 2391−2403.

Tamm, L. K. (1991) *Biochim. Biophys. Acta 1071*, 123−148.

Tomazin, R., Hill, A. B., Jugovic, P., York, I., Van Endert, P., Ploegh, H. L., Andrews, D. W., & Johnson, D. C. (1996) *EMBO J. 15*, 3256−3266.

Townsend, A., & Bodmer, H. (1989) *Annu. Rev. Immunol. 7*, 601−624.

Uebel, S., Meyer, T. H., Kraas, W., Kienle, S., Jung, G., Wiesmuller, K. H., & Tampé, R. (1995) *J. Biol. Chem. 270*, 18512−18516.

van Endert, P. M., Tampé, R., Meyer, T. H., Tisch, R., Bach, J. F., & McDevitt, H. O. (1994) *Immunity 1*, 491−500.

Watson, R. J., Umene, K., & Enquist, L. W. (1981) *Nucleic Acids Res. 9*, 4189−4199.

Whitton, J. L., & Clements, J. B. (1984) *J. Gen. Virol. 65*, 451−466.

Wimley, W. C., Creamer, T. P., & White, S. H. (1996) *Biochemistry 35*, 5109−5124.

Yewdell, J. W., & Bennink, J. R. (1992) *Adv. Immunol. 52*, 1−123.

Yin, Y., Zwang, F., Ling, V., & Arrowsmith, C. (1995) *FEBS Lett. 366*, 1−5.

Yorek, M. A. (1993) *Phospholipids handbook* (Cevc, G., Ed.) Marcel Dekker Inc., New York.

York, I. A., Roop, C., Andrews, D. W., Riddell, S. R., Graham, F. L., & Johnson, D. C. (1994) *Cell 77*, 525−35.

Zhang, F., Greig, D., & Ling, V. (1993) *Proc. Natl. Acad. Sci. U.S.A. 90*, 4211−4215.

Zhang, F., Arrowsmith, C. H., & Ling, V. (1995) *Biochemistry 34*, 4193−4201.

BI962940V